Calcium activates purified human TRPA1 with and without its N-terminal ankyrin repeat domain in the absence of calmodulin

Lavanya Moparthi, Satish Babu Moparthi, Jérôme Wenger, Peter M Zygmunt

Cell Calcium 90 (2020) 102228

Contents lists available at ScienceDirect

Cell Calcium

journal homepage: www.elsevier.com/locate/ceca

Calcium activates purified human TRPA1 with and without its N-terminal ankyrin repeat domain in the absence of calmodulin

Lavanya Moparthi[a,b], Satish Babu Moparthi[c,*], Jérôme Wenger[d], Peter M. Zygmunt[e,*]

[a] Wallenberg Centre for Molecular Medicine, Linköping University, SE-581 83, Linköping, Sweden
[b] Department of Biomedical and Clinical Sciences (BKV), Faculty of Health Sciences, Linköping University, SE-581 83, Linköping, Sweden
[c] Membrane Biochemistry and Transport, Institut Pasteur, 28 Rue Du Dr Roux, 75015, Paris, France
[d] Aix Marseille Univ, CNRS, Ecole Centrale Marseille, Institut Fresnel, 13013, Marseille, France
[e] Department of Clinical Sciences Malmö, Lund University, SE-214 28, Malmö, Sweden

ARTICLE INFO

Keywords:
Calcium
Calmodulin
TRP channel
TRPA1
Pain

ABSTRACT

Extracellular influx of calcium or release of calcium from intracellular stores have been shown to activate mammalian TRPA1 as well as to sensitize and desensitize TRPA1 electrophilic activation. Calcium binding sites on both intracellular N- and C-termini have been proposed. Here, we demonstrate based on Förster resonance energy transfer (FRET) and bilayer patch-clamp studies, a direct calmodulin-independent action of calcium on the purified human TRPA1 (hTRPA1), causing structural changes and activation without immediate subsequent desensitization of hTRPA1 with and without its N-terminal ankyrin repeat domain (N-ARD). Thus, calcium alone activates hTRPA1 by a direct interaction with binding sites outside the N-ARD.

1. Introduction

The mammalian pain receptor TRPA1 was initially identified as a noxious cold sensor and chemoreceptor of electrophilic irritants as well as non-electrophilic cannabinoids [1–3]. Importantly, TRPA1 was also shown to be activated by an increase in the intracellular free calcium concentration [2]. Whereas electrophiles are believed to promote TRPA1 channel opening primarily by binding to cysteine residues within the cytoplasmic N-terminus, the mechanism by which calcium modulates TRPA1 activity is not obvious [4–7]. Studies have shown a direct activation of TRPA1 by calcium in cell-membrane inside-out patches containing heterologously expressed TRPA1 [8–10]. However, an effect solely by calcium has been questioned as membrane bound calcium co-mediators such as calmodulin may still be present in isolated membrane patches [11]. Some studies have focused on the modulatory role of calcium on electrophilic TRPA1 activation, and also with regard to calmodulin dependence [11–15]. Furthermore, structures within the intracellular N- and C-termini have been suggested to contain calcium binding sites coupled to the gating of TRPA1 [9–11,13,15]. Interestingly, a calcium binding amino acid cluster has been identified in the C-terminus, and recently in the cytoplasmic end of transmembrane domain 2 and 3 of TRPA1 [13,15,16]. Clearly, further studies are needed to better understand the dynamics behind calcium modulation and activation of TRPA1.

In this study, we asked if calcium alone modifies the structure and induces activation of the purified hTRPA1 and Δ1-688 hTRPA1 without the N-terminal ankyrin repeat domain (N-ARD) (Fig. 1A). We report, based on Förster resonance energy transfer (FRET) and bilayer patch-clamp studies of purified hTRPA1 with and without its N-ARD, a direct non-calmodulin-dependent action of calcium on hTRPA1, causing structural changes and channel activity.

2. Materials and methods

2.1. Recombinant protein expression and purification

The hTRPA1 and Δ1-688 hTRPA1 were expressed in *Pichia pastoris* and purified as described earlier [17]. The purity of recombinant proteins was checked by SDS/PAGE followed by Coomassie Blue R-250 staining and mass spectrometry. The concentrations of all proteins were calculated using Bradford assays. For all experiments, His-tagged recombinant hTRPA1 proteins were used as it was shown that His-tagged

Abbreviations: FRET, Förster resonance energy transfer; N-ARD, N-terminal ankyrin repeat domain; TRP, Transient receptor potential; TRPA1, transient receptor potential ankyrin 1; hTRPA1, human TRPA1; FCS, Fluorescence correlation spectroscopy; A-967079, (1*E*3*E*)-1-(4-Fluorophenyl)-2-methyl-1-pentene-3-one oxime; HC030031, 2-(1,3-Dimethyl-2,6-dioxo-1,2,3,6-tetrahydro-7*H*-purin-7-yl)-*N*-(4-isopropylphenyl)acetamide

* Corresponding authors.
E-mail addresses: satish.moparthi@pasteur.fr (S.B. Moparthi), peter.zygmunt@med.lu.se (P.M. Zygmunt).

https://doi.org/10.1016/j.ceca.2020.102228
Received 23 April 2020; Received in revised form 26 May 2020; Accepted 2 June 2020
Available online 08 June 2020

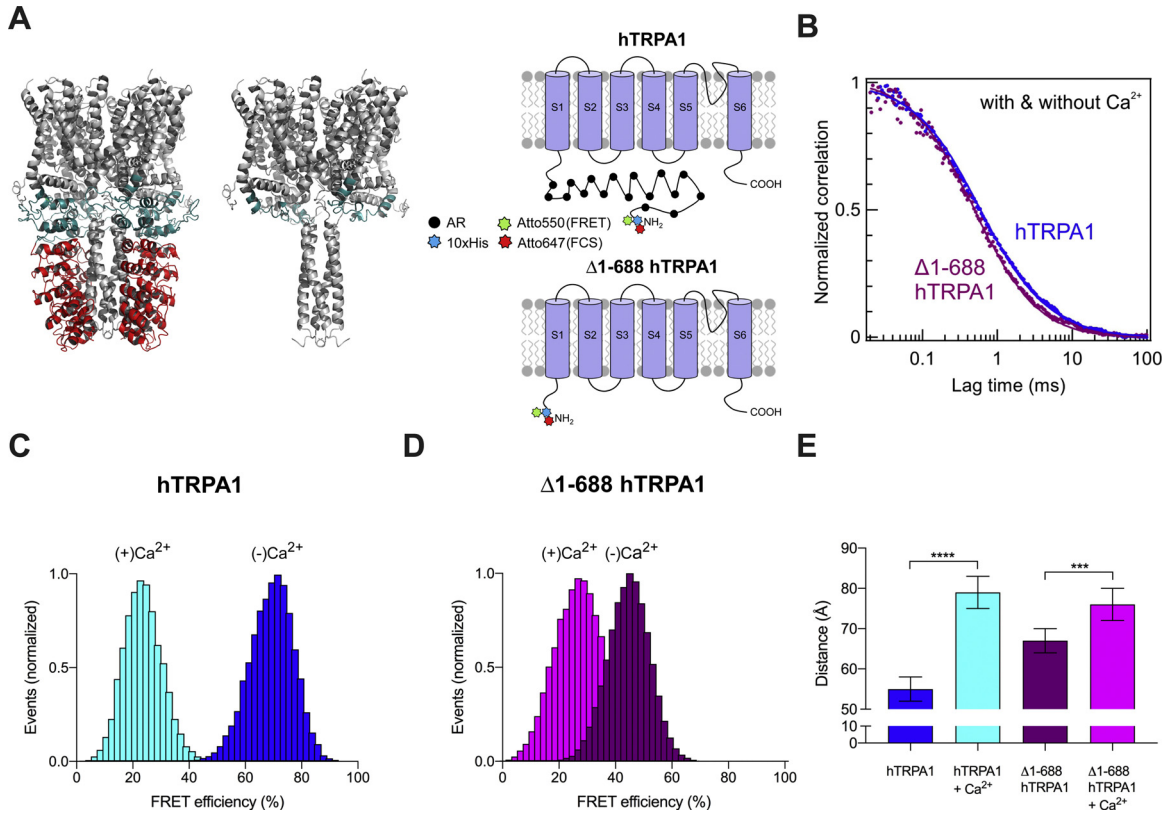

Fig. 1. Structural rearrangements of hTRPA1 with and without its N-terminal ARD (Δ1-688 hTRPA1) by calcium. (A) Tetrameric structure of hTRPA1 with and without its N-terminal ankyrin repeat domain (N-ARD) highlighted in red; Protein Data Bank (PDB) accession number 3J9P. Schematic representation of the full length hTRPA1 monomer and truncated Δ1-688 hTRPA1 monomer lacking ankyrin repeats (AR). The N-terminus His-tag was labeled with the fluorophore Atto647N and Atto550 in FCS and FRET experiments, respectively. (**B**) Normalised Fluorescence Correlation Spectroscopy (FCS) traces of hTRPA1 and Δ1-688 hTRPA1. Similar traces were obtained in presence and absence of 2 mM calcium, indicating that calcium did not noticeably modify the hydrodynamic radius monitored in FCS. (**C-E**) Single-molecule Förster Resonance Energy Transfer (FRET) efficiency histograms of intramolecular fluorophore dual-labeled (N-His-tag = Atto550 and lysines = Atto647 N) hTRPA1 (**C**) and Δ1-688 hTRPA1 (**D**) in the absence and presence 200 μM calcium. Gaussian and lognormal distributions are used to fit the data, and a higher value in FRET histograms indicates a higher degree of compactness of the protein. (**E**) Calculated average donor-acceptor intramolecular distance in ångström (Å) obtained from the FRET data in (**C**) and (**D**). Data is the mean ± SD of 5 (**B**) and 3 (**E**) separate experiments. ***$P < 0.001$ and ****$P < 0.0001$, Student's unpaired *t*-test. All experiments were performed at 22 °C after pre-incubation with calcium for 2 h at 22 °C.

hTRPA1 behaves like the native protein when expressed in HEK293 cells, indicating that the His-tag does not interfere in our experiments [17].

2.2. Protein labeling

In FCS experiments, the hTRPA1 and the Δ1-688 hTRPA1 N-terminal-His-tag was labeled with the Ni-NTA (Nα,Nα-bis(carboxymethyl)-L-lysine, Nickel(II) Atto647 N (Sigma-Aldrich) following the protocol provided by the manufacturer. In FRET experiments, the N-terminal-His-tag was labeled with the Ni-NTA Atto550 donor fluorophore (Sigma-Aldrich) and the lysine residues were labeled with the acceptor ATTO647 N succinimidyl ester (NHS ester) following the protocol provided by the manufacturer. Hence for the FRET experiments, a single fluorescent ATTO550 donor is present on the N-terminal while potentially multiple ATTO647 N acceptors are labeled on different lysine residues. In all cases, excess fluorophore was added to the aqueous protein solution containing 50 mM PBS buffer at pH 7.8 supplemented with 130 mM NaCl and 0.014 % phosphatidyl choline (FC14) (Sigma) and left for 8 h at 4 °C. The labeled protein was subsequently purified using size exclusion chromatography on a Sephadex™ G-25 Medium column (GE Healthcare, UK). To remove excess free dyes from the labeled proteins and also avoid hydrolysis of extra fluorophore, the samples were dialysed (3k membrane) for two times, four hours of incubation in each time at 4 °C. For long storage, the conjugates were divided into small aliquots frozen at 20 °C to avoid repeated freezing and thawing.

2.3. Sample preparation

In Fluorescence correlation spectroscopy (FCS) experiments, the concentration of the Atto647 N labeled hTRPA1 and Δ1-688 hTRPA1 in the measuring buffer was 50 nM and 2 mM of $CaCl_2$, both of which were incubated together for 2 h at 22 °C. In FRET experiments, the concentration of the Atto550/Atto647 N double-labeled hTRPA1 and Δ1-688 hTRPA1 was 10 nM and 200 μM of $CaCl_2$, both of which were incubated together for 2 h at 22 °C. The freshly prepared samples were immediately used for FCS and FRET experiments. In both assays, 0.1 % Tween-20 (Sigma) was added in order to diminish surface interactions with the glass coverslip.

2.4. Fluorescence correlation spectroscopy (FCS)

The FCS experiments were carried out at 22 °C with a custom-built confocal fluorescence microscope with a Zeiss C-Apochromat 40 × 1.2 NA water-immersion objective. The fluorescence intensity temporal fluctuations were analyzed with a hardware correlator (Flex02-12D/C correlator with 12.5 ns minimum channel width). All the experimental data were fitted by considering a single species and free Brownian 3D diffusion in the case of a Gaussian molecular detection efficiency:

$$g^{(2)}(\tau) = 1 + \frac{1}{N}\cdot\left(1 + n_T\cdot exp\left(-\frac{\tau}{\tau_T}\right)\right)\cdot\frac{1}{\left(1+\frac{\tau}{\tau_d}\right)\sqrt{1+s^2\left(\frac{\tau}{\tau_d}\right)}} \quad (1)$$

where N is the average number of molecules in the focal volume, n_T is the amplitude of the dark state population, τ_T is the dark state blinking time, τ_d is the mean diffusion time and s is the ratio of transversal to axial dimensions of the analysis volume. The molecular diffusion coefficient, D and hydrodynamic radius, R_H were calculated as previously described in detail [18]. The confocal volume was defined by using the 30 μm confocal pinhole conjugated to the sample plane whose transversal waist w_{xy} was calibrated to 285 nm using the known diffusion coefficient of Alexa 647 in pure water (3.1×10^{-6} $cm^2 \cdot s^{-1}$ at 22 °C) and known hydrodynamic radius of 0.7 nm in pure water. Each FCS measurement lasted for 100 s, and measurements were repeated several times on different days to determine the average translational diffusion times.

2.5. Förster resonance energy transfer (FRET)

The FRET signal was detected using a confocal inverted microscope with a Zeiss C-Apochromat 63 × 1.2 NA water-immersion objective, and an iChrome-TVIS laser (Toptica GmbH) as an exciting source operating at 550 nm. Filtering the laser excitation was achieved by a set of two bandpass filters (Chroma ET525/70 M and Semrock FF01-550/88). Dichroic mirrors (Chroma ZT594RDC and ZT633RDC) separate the donor and acceptor fluorescence light. The excitation power at the diffraction limited spot was set to 20 μW for all experimental conditions. The detection was performed by two avalanche photodiodes (Micro Photon Devices MPD-5CTC with 50 μm active surface) with 620 ± 20 nm (Chroma ET605/70 M and ET632/60 M) and 670 ± 20 nm (Semrock FF01-676/37) fluorescence bandpass filters for the donor and acceptor channels respectively. The photodiode signal was recorded by a fast time-correlated single photon counting module (Hydraharp400, Picoquant GmbH) in time-tagged time-resolved (TTTR) mode. Conceptually, the apparent FRET efficiency of each burst was calculated as previously described in detail [19]. All fluorescence bursts above the background noise were recorded separately by the acceptor channel and donor channel. As a part of calibration, we took into consideration the differences in the fluorescence detection efficiencies (η_A and η_D), direct excitation of the acceptor by the laser light (n_A^{de}), donor emission crosstalk into the acceptor channel (α) and quantum yields of fluorophores (φ_A and φ_D). Symphotime 64 (Picoquant GmbH) software was used to compute the FRET efficiency according to the formula below:

$$E = \frac{n_A - \alpha n_D - n_A^{de}}{n_A - \alpha n_D - n_A^{de} + \gamma n_D} \quad (2)$$

where $\gamma = \eta_A\varphi_A/\eta_D\varphi_D$ accounts for the differences in quantum yields (φ_A and φ_D) and fluorescence detection efficiencies (η_A and η_D) between the acceptor and donor.

We estimate $\gamma = 1.3$, and $\alpha = 0.16$ for the current setup.

2.6. Planar lipid bilayer patch-clamp electrophysiology

These experiments were performed as previously described in detail [17] and are briefly described as follows. Purified hTRPA1 and Δ1-688 hTRPA1 were reconstituted into preformed planar lipid bilayers composed of 1,2-diphytanoyl-sn-glycero-3-phosphocholine (Avanti Polar Lipids) and cholesterol (Sigma-Aldrich) in a 9:1 ratio and produced by using the Vesicle Prep Pro Station (Nanion Technologies). Ion channel activity was recorded at room temperature (20 − 22 °C) using the Port-a-Patch (Nanion Technologies) either by 2-s voltage-ramps (-100 to +100 mV) or at a holding potential (Vh) of +60 mV in a symmetrical K^+ solution (50 mM KCl, 10 mM NaCl, 60 mM KF, 20 mM EGTA, and 10 mM Hepes; adjusted to pH 7.2 with KOH), and with free Ca^{2+} concentrations calculated by MaxChelator (https://somapp.ucdmc.ucdavis.edu/pharmacology/bers/maxchelator/downloads.htm). Signals were acquired with an EPC 10 amplifier and PatchMaster software (HEKA) at a sampling rate of 50 kHz. Electrophysiological data were analyzed using Clampfit 9 (Molecular Devices) and Igor Pro (WaveMetrics). Data were processed by a Gaussian low-pass filter at 1000 Hz for analysis and 500 Hz for traces. The total number of functional channels (N) in the bilayer was determined by the number of peaks detected on all-points amplitude histograms. The relative open probability (NP_o) was obtained using the single-channel search function in Clampfit 9. The single-channel open probability (P_o) was calculated by dividing NP_o by the number of channels present in the bilayer. The single-channel conductance (G_s) was obtained from Gaussian fit of all-points amplitude histograms.

2.7. Statistics

GraphPad Prism 7.0. (GraphPad Software, La Jolla, CA) was used for statistical analysis and drawing of graphs. The level of statistical significance was set at $P < 0.05$. Comparisons between two groups of data were performed using Student's *t*-test or Mann-Whitney U-test. Data are presented as the mean ± SD or SEM; *n* indicates the number of separate experiments examined.

3. Results

3.1. Effect of calcium on hTRPA1 structure analyzed by FCS and FRET

Fluorescence Correlation Spectroscopy (FCS) monitors the average diffusion time of the protein across a fixed femtoliter detection volume. From the FCS data, the diffusion coefficient and the hydrodynamic radius can be obtained from the Stokes-Einstein equation. The FCS data recorded for hTRPA1 and Δ1-688 hTRPA1 indicate monophasic correlation curves with diffusion times of 560 ± 40 μs ($D = 3.6 \times 10^{-7}$ $cm^2 \cdot s^{-1}$) and 500 ± 30 μs ($D = 4.1 \times 10^{-7}$ $cm^2 \cdot s^{-1}$), respectively, in aqueous solution (Fig. 1B). The corresponding hydrodynamic radii are 6.2 nm for hTRPA1 and 5.6 nm for Δ1-688 hTRPA1. Faster diffusion time and smaller hydrodynamic radius for the truncated Δ1-688 hTRPA1 as compared to the full length hTRPA1 is in line with the lack of the N-terminal ankyrin repeat domain for the truncated protein. However, the FCS data did not reveal any major change in the presence or absence of calcium for both protein systems. We relate this effect to the fact that FCS is only sensitive to the average hydrodynamic radius of the system and lacks more accurate resolution on the protein conformation.

To gain more insight in the possible structural changes induced by calcium, we used intramolecular FRET between donor and acceptor dyes labelled within the protein. The effect of calcium on hTRPA1 and Δ1-688 hTRPA1 is clearly evidenced in the FRET energy transfer efficiency (*E*) histograms (Fig. 1C, D). In the absence of calcium, hTRPA1 displayed an average FRET efficiency $E = 0.72$, equivalent to a global distance of 55 ± 5 Å between the intramolecular donor and acceptor fluorophores (Fig. 1C, E). In the presence of calcium, hTRPA1 changed its structure significantly as indicated by $E = 0.24$, corresponding to a global distance of 79 ± 5 Å between the donor and acceptor fluorophores (Fig. 1C, E). Likewise, calcium increased the global distance between the Δ1-688 hTRPA1 intramolecular donor and acceptor fluorophores; $E = 0.45$ and at $E = 0.28$, in the absence and presence of calcium, respectively, corresponding to a calcium-evoked increase in global distance from 67 ± 5 Å to 76 ± 5 Å (Fig. 1D, E). Importantly, the fraction of samples containing only the donor dye was negligible in these experiments, as illustrated by the absence of only-donor peak centered at $E = 0$.

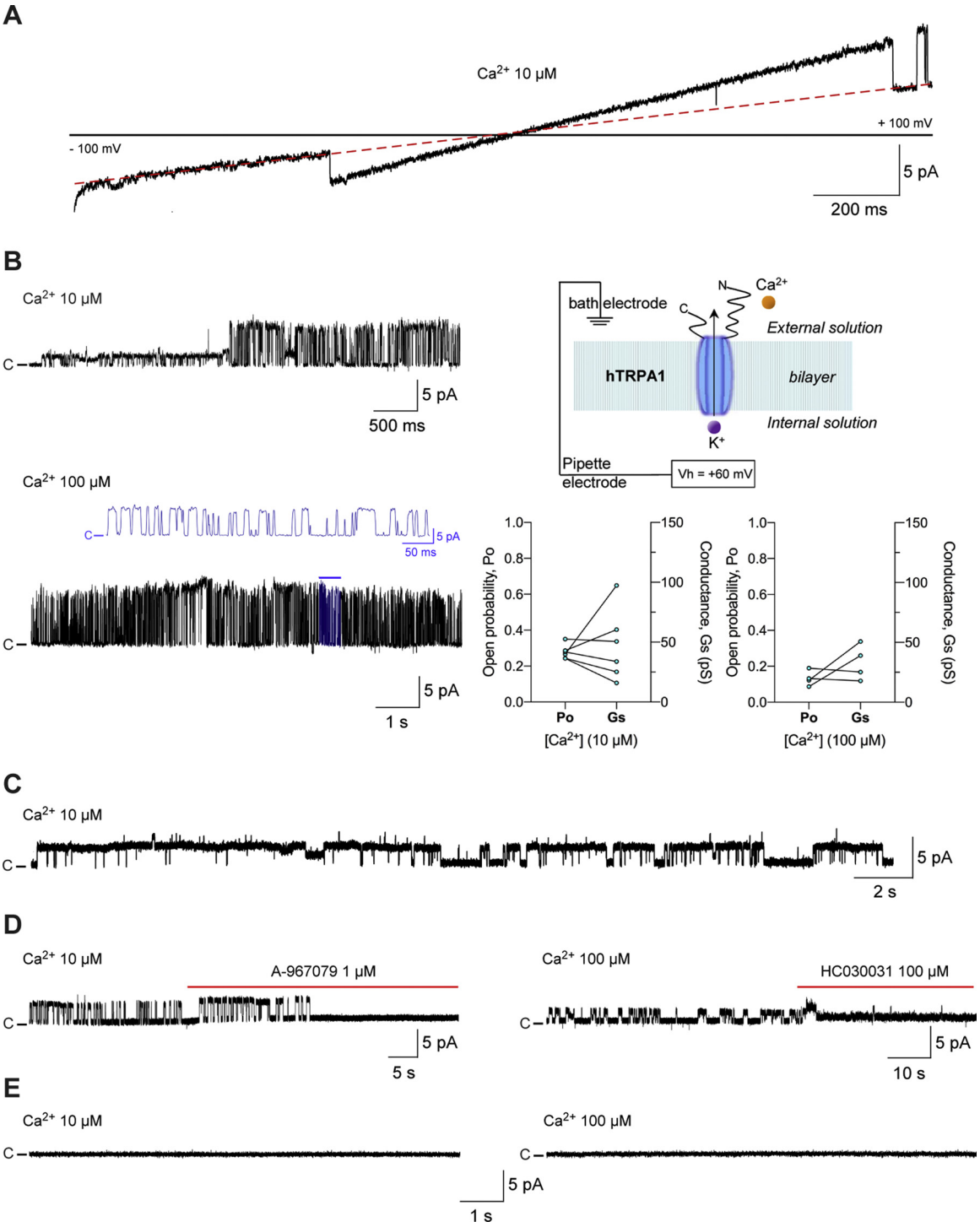

Fig. 2. Activation of human TRPA1 by calcium. Purified hTRPA1 was reconstituted into planar lipid bilayers and single-channel currents were recorded with the patch-clamp technique in a symmetrical K^+ solution at 20-22 °C. (**A**) Exposure to calcium (10 µM) evoked channel currents at both negative and positive test potentials (black trace) when recorded in 2-s voltage ramps from -100 to +100 mV (n = 3). Red dotted line shows zero channel current level. (**B**) As shown by representative traces, exposure to calcium triggered hTRPA1 outward single-channel currents of various magnitude and frequency at a holding potential (Vh) of +60 mV. Blue trace and bar show part of the recording (500 ms) at a higher time resolution. Under these conditions, a uniform protein orientation is favored with N- and C-termini facing the recording chamber (i.e., the "cytosolic compartment"). Graphs show calculated single-channel open probability and conductance values from 4-6 separate experiments. (**C** and **D**) No inactivation was observed within 30-60 s of exposure to calcium (n = 4). (**D**) Traces showing inhibition of calcium-evoked hTRPA1 activity by the TRPA1 antagonists A-967079 and HC030031 (n = 3). (**E**) Traces showing lack of calcium responses in the absence of hTRPA1 but in presence of its detergent Fos-Choline-14 at Vh +60 mV (each n = 5). C = closed-channel state. Open channel state = upward or downward deflection (**A**) and upward deflection (**B, C** and **D**).

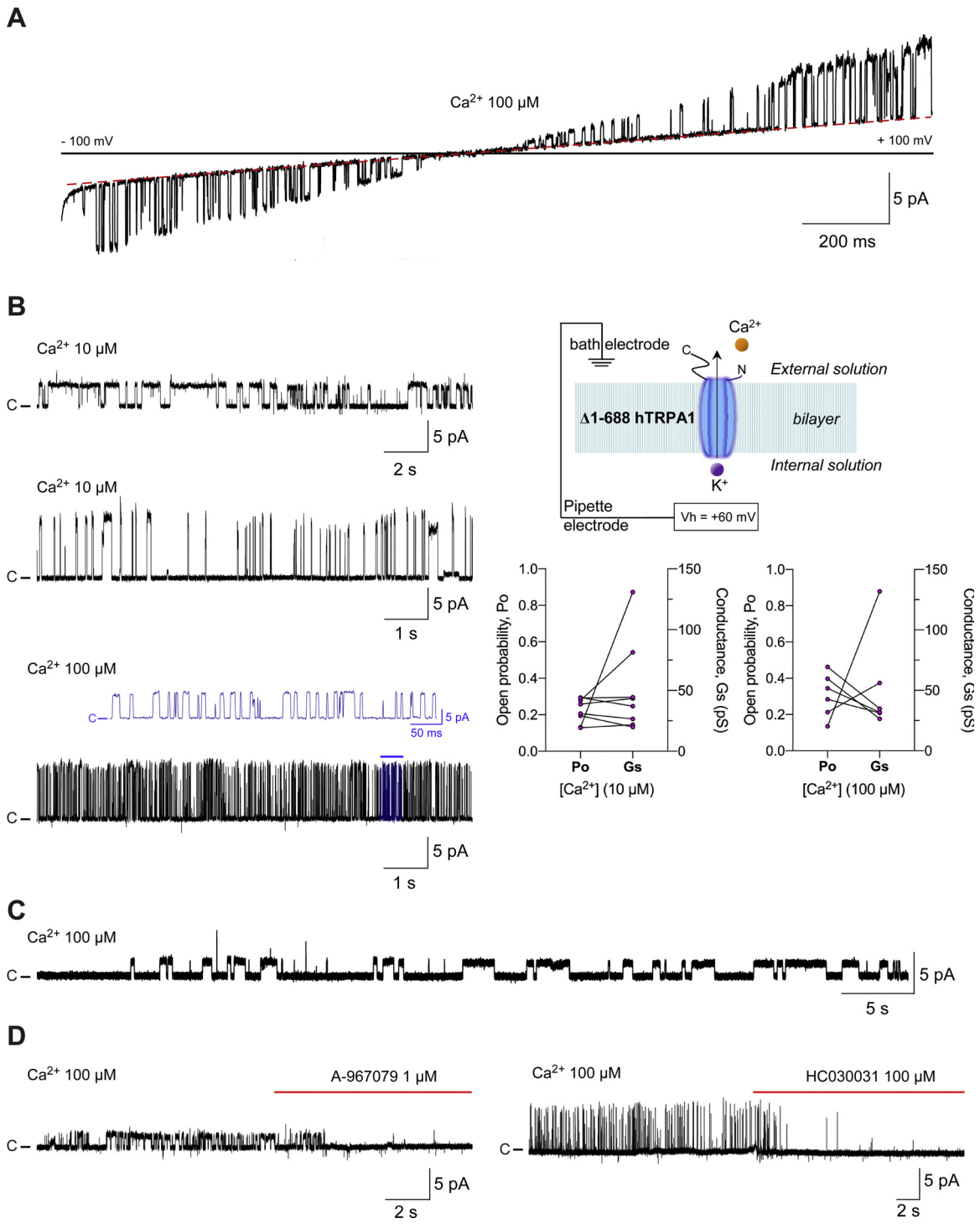

Fig. 3. Activation by calcium of human TRPA1 without its N-terminal ARD (Δ1-688 hTRPA1). Purified Δ1-688 hTRPA1 were reconstituted into planar lipid bilayers and single-channel currents were recorded with the patch-clamp technique in a symmetrical K^+ solution at 20-22 °C. (**A**) Exposure to calcium (100 µM) evoked channel currents at both negative and positive potentials (black trace) when recorded in 2-s voltage ramps from -100 to +100 mV (n = 3). Red dotted line shows zero channel current level. (**B**) As shown by representative traces, exposure to calcium triggered Δ1-688 hTRPA1 outward single-channel currents of various magnitude and frequency at a holding potential (Vh) of +60 mV. Blue trace and bar show part of the recording (500 ms) at a higher time resolution. Under these conditions, a uniform protein orientation is favored with N- and C-termini facing the recording chamber (i.e., the "cytosolic compartment"). Graphs show calculated single-channel open probability and conductance values from 6-8 separate experiments. (**C**) No inactivation was observed within 60 s of exposure to calcium (n = 4). (**D**) Traces showing inhibition of calcium-evoked hTRPA1 activity by the TRPA1 antagonists A-967079 and HC030031 (n = 3). C = closed-channel state. Open channel state = upward or downward deflection (**A**) and upward deflection (**B, C** and **D**).

3.2. Effect of calcium on hTRPA1 channel activity

The purified hTRPA1 and Δ1-688 hTRPA1 were reconstituted into artificial lipid bilayers for electrophysiological recordings of channel activity. As previously shown, a uniform protein orientation for hTRPA1 and Δ1-688 hTRPA1 is favored with N- and C-termini facing the recording chamber [17], and thus both hTRPA1 proteins are exposed to "intracellular" calcium in the present study (Figs. 2 and 3).

Under these conditions, hTRPA1 and Δ1-688 hTRPA1 responded to calcium (10 and 100 μM) with vivid channel behavior including various single-channel current levels (Figs. 2 and 3). However, there was no obvious link between matched single-channel open probability and conductance levels for both hTRPA1 proteins (Figs. 2B and 3 B). The single-channel open probability values for hTRPA1 and Δ1-688 hTRPA1 were different at 100 μM calcium (0.13 ± 0.021 for hTRPA1vs 0.31 ± 0.049 for Δ1-688 hTRPA1; n = 4–6, P = 0.0190, Mann-Whitney U-test). There was no sign of channel inactivation within 30–60 sec of recording for hTRPA1 (Fig. 2C, D; n = 4) and Δ1-688 hTRPA1 (Fig. 3C; n = 4). The activity of hTRPA1 and Δ1-688 hTRPA1 was abolished by the TRPA1 antagonists A-967079 and HC030031 (Fig. 2D and 3D), both obtained from Sigma-Aldrich. A-967079 inhibits hTRPA1 with an IC_{50} value of 67 nM and is about 100 times more potent than HC030031 [20,21], which was used in this study at a concentration that abolished purified hTRPA1 and Δ1-688 hTRPA1 single-channel activity evoked by chemical ligands, temperature and mechanical stimuli [17,22–24]. Furthermore, in "knock-out" experiments, i.e., membranes without the purified hTRPA1 proteins, no channel activity was observed in response to 10 and 100 μM of calcium (Fig. 2E). No basal TRPA1 activity was observed at 20 − 22 °C (not shown), as also reported by numerous previous observations [17,22–24].

4. Discussion

The effect of calcium on TRPA1 is mechanistically intriguing, and encompasses channel activation by calcium alone as well as calcium channel sensitization/desensitization of ligand activation [5–7]. These effects of calcium may occur by a direct interaction with TRPA1 or as a result of association with a calcium binding partner such as calmodulin [8–11,13–16]. The site of action may be on the cytoplasmic N- and C-termini [5]. In this, study, we have addressed the possibility of a direct interaction between calcium and purified hTRPA1 without any interplay with other calcium-sensitive proteins including calmodulin, TRPV1 and A-kinase anchoring protein (AKAP) that can associate with TRPA1 and influence its function [5,7,15].

As shown in FRET experiments, the FRET efficiency distributions of both hTRPA1 and Δ1 − 688 drastically changed in the presence of 200 μM calcium, indicating structural rearrangements caused by a direct interaction between calcium and channel structures outside the N-ARD. The FCS experiments confirmed that all samples contained the same number of fluorescently-labeled hTRPA1 molecules in the confocal volume under the various experimental conditions. Furthermore, when 2 μM of non-labeled hTRPA1 proteins were added to 50 nM of labeled hTRPA1 proteins, the same fluorescence brightness and similar hydrodynamic radii were observed as in the absence of non-labeled TRPA1 proteins. These results indicate that in vitro there is no substantial shuffling between the labeled and non-labeled hTRPA1 monomers, and thus both hTRPA1 and Δ1 − 688 hTRPA1 exist as a stable tetramer complex in the aqueous test solution. Although it could be argued that the changes in FRET efficiency induced by calcium is due to the formation of TRPA1 aggregates formed by intermolecular interactions [25], the fluorescence intensity traces showed no signs of aggregates. In spite of a random labeling of lysines, both hTRPA1 and Δ1-688 hTRPA1 showed a similar donor-acceptors global distance of 79 Å and 76 Å, respectively, in the presence of calcium, possibly suggesting that intramolecular repulsions were the same in both hTRPA1 proteins and that calcium may share similar binding sites in hTRPA1 and Δ1-688 hTRPA1.

To gain further insight into the functional consequences of calcium-induced structural changes of hTRPA1 with and without its N-ARD, we reconstituted the purified hTRPA1 proteins into artificial lipid bilayers, with a uniform protein orientation similar to inside-out cell membrane patches, for recording of electrical activity as in our previous studies of hTRPA1 intrinsic chemo- thermo- and mechanosensitivity [17,22–24]. As shown in voltage-ramp recordings, calcium evoked channel activity at both positive and negative potentials, which is in line with ligand and temperature stimulation of purified hTRPA1 and Δ1-688 hTRPA1 [17,23]. If calcium activates purified hTRPA1 in a voltage- and N-ARD-dependent manner as shown for electrophilic and non-electrophilic activators [17] is clearly of interest to find out, also because hTRPA1 calcium activation and voltage are closely linked [9,10,13,26], but a topic for future studies. At calcium concentrations that evoked half and near maximal activation of heterologously expressed TRPA1 in whole cells and isolated inside-out cell membrane patches [8–10], we recorded intense activity of both hTRPA1 and Δ1-688 hTRPA1 at a holding potential of +60 mV. In comparison with the activation of purified hTRPA1 by most ligands and temperature [17,22,23], under the same experimental conditions, calcium seemed to evoke more variability in channel behaviour. Considering the many possible calcium binding sites on TRPA1 [9–11,13,15,16], it could be speculated that calcium hits TRPA1 at multiple binding sites synergistically causing dynamic pore conformational changes and the variability in single-channel behavior as observed in this study. Therefore, it seems reasonable that intracellular co-factors such as calmodulin tightly control and fine-tune the otherwise wild action of calcium on TRPA1 [11,15]. Our aim was not to study calcium sensitization/desensitization properties of hTRPA1 by calcium alone or in the presence of TRPA1 activators such as cinnamaldehyde and AITC, but we noticed a lack of calcium self-desensitization in recordings between 30–60 sec, which is in contrast to recordings in excised inside-out cell membrane patches within the same timeframe [9,14]. This discrepancy could indicate that there are still TRPA1 channel modifiers present in isolated patches of the cell membrane that complicate studies of a direct interaction between calcium and TRPA1, as discussed by Hasan and colleagues [11]. Importantly, in a mass spectrometry study on hTRPA1 and Δ1-688 hTRPA1 [27], we did not find any calcium binding partners including calmodulin associated with hTRPA1 and Δ1-688 hTRPA1, which could have been reminiscent of the expression and purification of the hTRPA1 proteins performed in *Pichia pastoris*. The higher open probability for hTRPA1 without its N-ARD at 100 μM calcium is interesting and could indicate that calcium modulates hTRPA1 activity also by interacting with a putative EF-hand calcium-binding domain in the N-terminus. This possibility could, however, not be tested as the hTRPA1 without its intracellular C-terminus does not express in *Pichia pastoris*. Importantly, the deletion of the N-ARD including the EF-hand like domain does not allow heterologous cell membrane expression of functional mammalian TRPA1 [6], and thus our strategy using purified Δ1-688 hTRPA1 offers a unique possibility to explore TRPA1 gating by calcium independent of the N-ARD as well as avoiding potential artificial effects on channel gating caused by N-ARD mutational and chimeric strategies [7]. Thus, our finding that calcium interacts with hTRPA1 outside the N-ARD is in agreement with studies suggesting specific calcium binding sites in the C-terminus and/or in the cytoplasmic end of transmembrane domain 2 and 3 of TRPA1 [13,15,16].

In conclusion, calcium directly interacts with hTRPA1 outside its N-ARD in a non-calmodulin-dependent manner, causing structural changes and hTRPA1 channel activity without immediate subsequent channel desensitization.

Author contributions

L.M., S.B.M., J.W. and P.M.Z. designed research; S.B.M. performed FCS and FRET experiments; L.M. purified hTRPA1 proteins and performed electrophysiology experiments; L.M., S.B.M., J.W. and P.M.Z. analyzed data; L.M., S.B.M., J.W. and P.M.Z. wrote the paper.

Declaration of Competing Interest

The authors declare no conflict of interest.

Acknowledgements

This study was supported by the Swedish Research Council (2014-3801) and the Medical Faculty of Lund University - ALF (Dnr. ALFSKANE-451751). This project has received funding from the Agence Nationale de la Recherche (ANR) under grant agreement ANR-17-CE09-0026-01 and from the European Research Council (ERC) under the European Commission's Seventh Framework Programme (grant agreement 278242).

References

[1] M. Bandell, G.M. Story, S.W. Hwang, V. Viswanath, S.R. Eid, M.J. Petrus, T.J. Earley, A. Patapoutian, Noxious cold ion channel TRPA1 is activated by pungent compounds and bradykinin, Neuron 41 (2004) 849–857.

[2] S.E. Jordt, D.M. Bautista, H.H. Chuang, D.D. McKemy, P.M. Zygmunt, E.D. Högestätt, I.D. Meng, D. Julius, Mustard oils and cannabinoids excite sensory nerve fibres through the TRP channel ANKTM1, Nature 427 (2004) 260–265.

[3] G.M. Story, A.M. Peier, A.J. Reeve, S.R. Eid, J. Mosbacher, T.R. Hricik, T.J. Earley, A.C. Hergarden, D.A. Andersson, S.W. Hwang, P. McIntyre, T. Jegla, S. Bevan, A. Patapoutian, ANKTM1, a TRP-like channel expressed in nociceptive neurons, is activated by cold temperatures, Cell 112 (2003) 819–829.

[4] Y. Suo, Z. Wang, L. Zubcevic, A.L. Hsu, Q. He, M.J. Borgnia, R.R. Ji, S.Y. Lee, Structural insights into electrophile irritant sensing by the human TRPA1 channel, Neuron 105 (5) (2019) 882–894, https://doi.org/10.1016/j.neuron.2019.11.023.

[5] K. Talavera, J.B. Startek, J. Alvarez-Collazo, B. Boonen, Y.A. Alpizar, A. Sanchez, R. Naert, B. Nilius, Mammalian transient receptor potential TRPA1 channels: from structure to disease, Physiol. Rev. 100 (2020) 725–803, https://doi.org/10.1152/physrev.00005.2019.

[6] B. Nilius, J. Prenen, G. Owsianik, Irritating channels: the case of TRPA1, J. Physiol. 589 (2011) 1543–1549, https://doi.org/10.1113/jphysiol.2010.200717.

[7] P.M. Zygmunt, E.D. Högestätt, Trpa1, Handb. Exp. Pharmacol. 222 (2014) 583–630, https://doi.org/10.1007/978-3-642-54215-2_23.

[8] E.J. Cavanaugh, D. Simkin, D. Kim, Activation of transient receptor potential A1 channels by mustard oil, tetrahydrocannabinol and Ca2+ reveals different functional channel states, Neuroscience 154 (2008) 1467–1476, https://doi.org/10.1016/j.neuroscience.2008.04.048.

[9] J.F. Doerner, G. Gisselmann, H. Hatt, C.H. Wetzel, Transient receptor potential channel A1 is directly gated by calcium ions, J. Biol. Chem. 282 (2007) 13180–13189, https://doi.org/10.1074/jbc.M607849200.

[10] S. Zurborg, B. Yurgionas, J.A. Jira, O. Caspani, P.A. Heppenstall, Direct activation of the ion channel TRPA1 by Ca^{2+}, Nat. Neurosci. 10 (2007) 277–279.

[11] R. Hasan, A.T. Leeson-Payne, J.H. Jaggar, X. Zhang, Calmodulin is responsible for Ca(2+)-dependent regulation of TRPA1 Channels, Sci. Rep. 7 (2017) 45098, https://doi.org/10.1038/srep45098.

[12] K. Nagata, A. Duggan, G. Kumar, J. Garcia-Anoveros, Nociceptor and hair cell transducer properties of TRPA1, a channel for pain and hearing, J. Neurosci. 25 (2005) 4052–4061.

[13] L. Sura, V. Zima, L. Marsakova, A. Hynkova, I. Barvik, V. Vlachova, C-terminal acidic cluster is involved in Ca2+-induced regulation of human transient receptor potential ankyrin 1 channel, J. Biol. Chem. 287 (2012) 18067–18077, https://doi.org/10.1074/jbc.M112.341859.

[14] Y.Y. Wang, R.B. Chang, H.N. Waters, D.D. McKemy, E.R. Liman, The nociceptor ion channel TRPA1 is potentiated and inactivated by permeating calcium ions, J. Biol. Chem. 283 (2008) 32691–32703, https://doi.org/10.1074/jbc.M803568200.

[15] L. Zimova, K. Barvikova, L. Macikova, L. Vyklicka, V. Sinica, I. Barvik, V. Vlachova, Proximal C-terminus serves as a signaling hub for TRPA1 channel regulation via its interacting molecules and supramolecular complexes, Front. Physiol. 11 (2020), https://doi.org/10.3389/fphys.2020.00189.

[16] J. Zhao, L. King, C.E. Paulsen, Y. Cheng, D. Julius, Mechanisms governing irritant-evoked activation and calcium modulation of TRPA1, BioRxiv (2019), https://doi.org/10.1101/2019.12.26.888982.

[17] L. Moparthi, S. Survery, M. Kreir, C. Simonsen, P. Kjellbom, E.D. Hogestatt, U. Johanson, P.M. Zygmunt, Human TRPA1 is intrinsically cold- and chemosensitive with and without its N-terminal ankyrin repeat domain, Proc. Natl. Acad. Sci. U. S. A. 111 (2014) 16901–16906, https://doi.org/10.1073/pnas.1412689111.

[18] S.B. Moparthi, G. Thieulin-Pardo, P. Mansuelle, H. Rigneault, B. Gontero, J. Wenger, Conformational modulation and hydrodynamic radii of CP12 protein and its complexes probed by fluorescence correlation spectroscopy, FEBS J. 281 (2014) 3206–3217, https://doi.org/10.1111/febs.12854.

[19] S.B. Moparthi, G. Thieulin-Pardo, J. de Torres, P. Ghenuche, B. Gontero, J. Wenger, FRET analysis of CP12 structural interplay by GAPDH and PRK, Biochem. Biophys. Res. Commun. 458 (2015) 488–493, https://doi.org/10.1016/j.bbrc.2015.01.135.

[20] J. Chen, S.K. Joshi, S. DiDomenico, R.J. Perner, J.P. Mikusa, D.M. Gauvin, J.A. Segreti, P. Han, X.F. Zhang, W. Niforatos, B.R. Bianchi, S.J. Baker, C. Zhong, G.H. Simler, H.A. McDonald, R.G. Schmidt, S.P. McGaraughty, K.L. Chu, C.R. Faltynek, M.E. Kort, R.M. Reilly, P.R. Kym, Selective blockade of TRPA1 channel attenuates pathological pain without altering noxious cold sensation or body temperature regulation, Pain 152 (2011) 1165–1172, https://doi.org/10.1016/j.pain.2011.01.049.

[21] C.R. McNamara, J. Mandel-Brehm, D.M. Bautista, J. Siemens, K.L. Deranian, M. Zhao, N.J. Hayward, J.A. Chong, D. Julius, M.M. Moran, C.M. Fanger, TRPA1 mediates formalin-induced pain, Proc. Natl. Acad. Sci. U. S. A. 104 (2007) 13525–13530, https://doi.org/10.1073/pnas.0705924104.

[22] A. Babes, S.K. Sauer, L. Moparthi, T.I. Kichko, C. Neacsu, B. Namer, M. Filipovic, P.M. Zygmunt, P.W. Reeh, M.J. Fischer, Photosensitization in porphyrias and photodynamic therapy involves TRPA1 and TRPV1, J. Neurosci. 36 (2016) 5264–5278, https://doi.org/10.1523/JNEUROSCI.4268-15.2016.

[23] L. Moparthi, T.I. Kichko, M. Eberhardt, E.D. Hogestatt, P. Kjellbom, U. Johanson, P.W. Reeh, A. Leffler, M.R. Filipovic, P.M. Zygmunt, Human TRPA1 is a heat sensor displaying intrinsic U-shaped thermosensitivity, Sci. Rep. 6 (2016) 28763, https://doi.org/10.1038/srep28763.

[24] L. Moparthi, P.M. Zygmunt, Human TRPA1 is an inherently mechanosensitive bilayer-gated ion channel, BioRxiv (2020), https://doi.org/10.1101/2020.03.05.979252.

[25] A. Krippner-Heidenreich, F. Tubing, S. Bryde, S. Willi, G. Zimmermann, P. Scheurich, Control of receptor-induced signaling complex formation by the kinetics of ligand/receptor interaction, J. Biol. Chem. 277 (2002) 44155–44163, https://doi.org/10.1074/jbc.M207399200.

[26] B. Kremeyer, F. Lopera, J.J. Cox, A. Momin, F. Rugiero, S. Marsh, C.G. Woods, N.G. Jones, K.J. Paterson, F.R. Fricker, A. Villegas, N. Acosta, N.G. Pineda-Trujillo, J.D. Ramirez, J. Zea, M.W. Burley, G. Bedoya, D.L. Bennett, J.N. Wood, A. Ruiz-Linares, A gain-of-function mutation in TRPA1 causes familial episodic pain syndrome, Neuron 66 (2010) 671–680, https://doi.org/10.1016/j.neuron.2010.04.030.

[27] L. Moparthi, Thermo- and Chemosensitive Properties of Transient Receptor Potential Ankyrin 1 Ion Channels, Thesis Lund University, 2016, http://lup.lub.lu.se/record/8837704.